2009 IEEE/ASME International Conference on Advanced Intelligent Mechatronics
Suntec Convention and Exhibition Center
Singapore, July 14-17, 2009

Automatic Centroid Detection for Shack-Hartmann Wavefront Sensor

Xiaoming Yin, Xiang Li, Liping Zhao and Zhongping Fang

Abstract—**Shark-Hartmann Wavefront sensor splits the incident wavefront into many subsections and transfers the distorted wavefront detection into the centroid measurement. The accuracy of the centroid measurement determines the accuracy of the Shack-Hartmann Wavefront Sensor. A lot of methods have been presented to improve the accuracy of the wavefront centroid measurement. However, most of these methods are discussed from the point of view of optics, and based on the assumption that the spot intensity of the SHWS has a Gaussian distribution, which is not applicable to the digital SHWS. In this paper, we have presented a new centroid measurement algorithm based on adaptive thresholding and dynamic windowing method by utilizing image processing techniques for practical application of the digital Shack-Hartmann Wavefront Sensor in surface profile measurement. The method can detect the centroid of the spot accurately and robustly by eliminating the influences of various noises such as diffraction of the digital SHWS, uneven and instability of the light source as well as deviation between the centroid of the spot and the center of the detection area. The experimental results demonstrate that the algorithm has better accuracy, repeatability and stability compared with other commonly used centroid methods such statistic averaging, thresholding and windowing algorithms.**

I. Introduction

Shack-Hartmann Wavefront Sensor (SHWS) samples the incident wavefront by means of a lenslet array which produces an array of spots on a detector. The wavefront is spatially sampled and focused by a micro-lenslet array on a suitable detector such as a CCD camera. This provides an array of focus spots, each corresponding to a sub-aperture sample data. The centroid of each sub-aperture sampled image is displaced from its mean position by an amount proportional to the tilt of the wavefront across the corresponding lenslet aperture. From the measurement of a local wavefront tilt, the wavefront deformation can be estimated by the wavefront reconstruction [1]. The accuracy of the SHWS for measuring the wavefront distortion is mainly dependent upon the measuring accuracy of the centroid of each spot.

The accuracy of the centroid detection is affected by many factors. The photon noise, the read-out noise of the detector, the background noise as well as the sampling and truncation error are the main error sources, and have been widely investigated theoretically and experimentally [2, 3, 4]. A lot of methods have also been presented to improve the accuracy of the centroid measurement. The statistical averaging algorithm, i. e. the center of mass, is most widely used method according to the definition of centroid. However, this method is sensitive to the influence of the noise, particularly in the case that the signal spot area is relatively small compared with the detection area. The common methods to overcome the influence of the noise are the thresholding and windowing algorithms [5, 6]. In the thresholding algorithm, a threshold is used to improve the Signal Noise Ratio (SNR). In the windowing algorithm, the detection window size is changed to reduce the influence of the noise. Based on these methods, other improved algorithms have been proposed. S. H. Baik et al [7] has presented a modified averaging method which uses some power from the photon events of each pixel instead of photon events themselves. This method led to the pixels near the spot's center having great effect on the calculation of the centroid. A wavelet-base approach for the measurement of moments in Shack-Hartmann sensor has been presented in [8]. The other methods such as maximum a posteriori algorithm, maximum-likelihood estimation, etc have been used to improve the estimation accuracy of the controid as well [9, 10].

A lot of work has also been devoted to study and compare the measurement accuracy of various centroid detection algorithms. J. Ares and J. Arines have presented a full analytical description of the interaction between centroiding and thresholding applied over an intensity distribution corrupted by additive Gaussion noise in [11]. Z. L. Jiang et al made a direct performance comparison of the averaging algorithm, the windowing algorithm, the thresholding algorithm and the weighted averaging algorithm in [12]. The influences of the detected window size, the threshold and the power factor on centroid measurement were investigated by Monte-Carlo simulation technology in their paper.

However, most centroid detection methods have been proposed and analyzed from the point of view of optics. And the accuracy of the methods has been studied only by simulation. In this paper, we have proposed a new centroid detection algorithm based on adaptive thresholding and dynamic windowing method for practical application of digital Shark-Hartmann wavefront sensor in surface measurement. In this method, we automatically detect the centroid of each focal spot using an adaptive threshold in a dynamical detection window by utilizing image processing techniques. We also study the accuracy, the stability and repeatability of the algorithm using real wavefront images.

X. Yin is with the Singapore Institute of Manufacturing Technology, 71 Nanyang Drive, Singapore 638075 (corresponding author to provide e-mail:xmyin@SIMTech.a-star.edu.sg).

X. Li, L. Zhao and Z. Fang are with the Singapore Institute of Manufacturing Technology, 71 Nanyang Drive, Singapore 638075.

II. Image Processing Based Centroid Detection Algorithm

A. Digital Shack-Hartmann Wavefront Sensor

We have developed a digital Shack-Hartmann Wavefront Sensor in which a Spatial Light Modulator (SLM) is employed to replace the conventional physical lenslet array used in SHWS. A SLM consists of an array of optical elements or pixels where each pixel can modulate the amplitude and phase of incident light. So the lenslet of the digital SHWS can be formed by programming of pixels of SLM based on the technique of Diffractive Optics Element (DOE). The focal length, size, pitch, format and layout of the lenslet array can be changed according to different applications. The dynamic range and accuracy of the digital SHWS will change accordingly and the adaptive measurement can be realized.

We have generated an 8×6 lenslet array with 60*mm* focal length at 633*nm* with a SLM for our experiment. The pattern of the diffractive lenslet array is shown in Fig. 1. The pixel size of the SLM is 32μm, the spacing between the lenslet is 30 pixels or 960μm, and the radius of the lenslet is 15 pixels or 480μm. Diffractive optical lenslets are uniformly distributed and the diameters of the lenslets are also the same. A CCD camera is applied to detect the array of focus spots. The resolution of the CCD is 768×572, and the pixel size is 8μm. Fig. 2 show the focus spots image detected by the CCD camera.

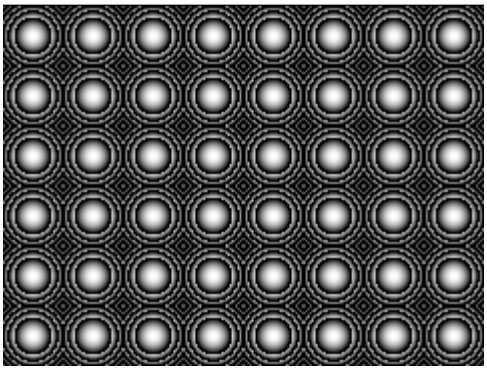

Fig. 1. Lenslet array generated with a Spatial Light Modulator.

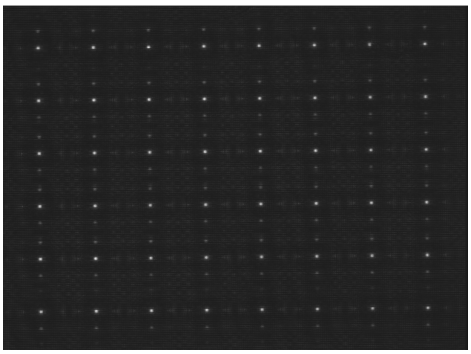

Fig. 2. Focus spots array detected by a CCD camera.

The diffractive lenslet array generated with SLM functioned well in the wavefront sensing system with greater flexibility and programmability compared with the traditional physical lenslet array. However, besides the focus spots, there are some bright dots observed on the focal plane as well, and stronger diffraction effect in the vertical direction is observed than in the horizontal direction, as shown in Fig. 2. These noisy diffraction dots cannot be eliminated practically due to the coherent light source used in our system. Such noise degrades the performance of the wavefront measurement and also makes centroid detection more difficult and inaccurate if using common centroid detection algorithms. In order to eliminate the effect of diffraction noise, we propose the following centroid detection algorithm based on adaptive thresholding and dynamic windowing method.

B. Determine Sub-areas of Spots

In most methods having been presented, the centroid is measured for only one sub-aperture from the image which is generated by simulation or detected by a CCD camera. The detection area is usually set as the corresponding region of the sub-aperture on the CCD. However, we can not consider only one sub-aperture in practical applications such as surface measurement. We also can not get the detection area of each sub-aperture by just dividing the image uniformly based on the size and number of sub-apertures, because the CCD may not be big enough to cover all the sub-apertures, or there is a shift or tilt of spot positions on the image.

In our method, we don't determine the detection area based on the exact dimension of the sub-aperture. Instead, we determine the detection area of each sub-aperture directly on the image. Based on the positions of focus spots in the image, we first determine the sub-areas of spots, then identify the detection area of each spot using the algorithms described in the following subsections. The size of the spot sub-area is defined manually without any strict limitation. The only requirement is that one sub-area should cover only one spot.

A centroid detection software system has been developed for our digital SHWS. The software can automatically generate the sub-area of each spot after the size of the sub-area and the position of the first sub-area has been defined, as shown in Fig. 3. So the sub-areas of spots are very easy to be defined in the image without need to know the physical properties of the lenslet array.

C. Detect Spots

The position of the spot has a strong influence on centroid calculation to common centroid detection algorithms such as statistic averaging and windowing algorithms. In the case that the centroid of the spot is not at the center of the detection area, these algorithms will result in a relatively high systemic error. Some algorithms locate the brightest pixel as the approximate center of the spot, but in the case of strong readout noise and weak signal, the brightest pixel may not be on the spot. When the spot is not detected, the centroid calculation with these methods is completely wrong.

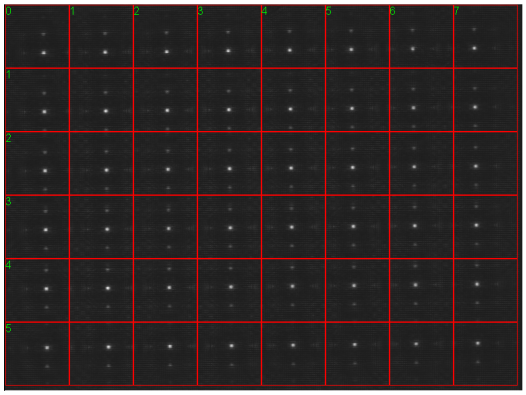

Fig. 3. Spot sub-areas defined directly in the image.

In our method, we propose the following algorithm to detect spots:

1. Find the n^{th} high intensity value I^n in the spot sub-area.
2. Use I^n as the threshold to binarize the image in the spot sub-area and select the biggest blob in the binary image as the spot.
3. Calculate the center of mass of the spot C_i as the approximate center of the spot.

Here, we don't find the highest intensity value, but the n^{th} high intensity value as the threshold. For example, the intensity value of a spot sub-area has the following distribution: 250, 248, 245, 230, 200, 150, 140…. If n is chosen as 4, the 4^{th} high intensity value is 230. So the intensity value of 230 is determined as the threshold to binarize the image in this spot sub-area. We don't set the threshold to a direct intensity value, because the intensity distribution of each spot sub-area may be different due to the uneven of the light source. It is difficult to find a single intensity value which can segment every spot image well in the case that the intensity of the whole image is not uniform.

Then the biggest blob after binarization is determined as the spot, and the center of mass of this blob is calculated as the approximate center of the spot. By using this method, the influence of those noises, which have relative high intensity value but small area, is eliminated.

D. Calculate Centroids

After the spots have been detected, the detection area of each spot centroid can be identified based on the spot center. The detection area is defined as a rectangular window surrounding the spot in the image, which is centered at the spot center. The size of the window can be set manually according to the area of the spot. The software can automatically generate the detection area of each spot based on the predefined size of the detection window after the spot center has been detected.

After that, the centroid of each spot is calculated using the thresholding method from the pixels within the detection window. The threshold is set as the same as I^n, the n^{th} high intensity value in the spot sub-area, which has been used as the threshold for spot detection in above section. The calculation equations are as follows

$$x_c = \frac{\sum_{i=1}^{U}\sum_{j=1}^{V}\left(I(i,j) - I^n\right)H(i,j)\cdot x_{ij}}{\sum_{i=1}^{U}\sum_{j=1}^{V}\left(I(i,j) - I^n\right)H(i,j)} \quad (1)$$

$$y_c = \frac{\sum_{i=1}^{U}\sum_{j=1}^{V}\left(I(i,j) - I^n\right)H(i,j)\cdot y_{ij}}{\sum_{i=1}^{U}\sum_{j=1}^{V}\left(I(i,j) - I^n\right)H(i,j)} \quad (2)$$

$$H(i,j) = \begin{cases} 1, I(i,j) \geq I^n \\ 0, I(i,j) < I^n \end{cases} \quad (3)$$

where x_c and y_c are the centroid position of the spot. $I(i,j)$ is the intensity value of the (i,j) pixel. I^n is the n^{th} high intensity value in this spot sub-area. x_{ij} and y_{ij} are the coordinates of the (i,j) pixel in the whole spot image. U and V are the numbers of the pixels along X and Y directions in the detection window.

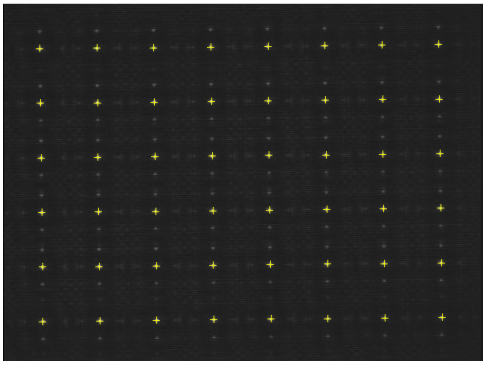

Fig. 4. Detected centroids of focus spots.

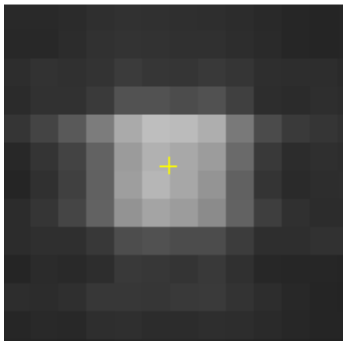

Fig. 5. Enlarged picture of one of centroids.

Fig. 4 shows the centroids of focus spots detected from the image shown in Fig. 2, and Fig. 5 shows the enlarged picture of one of centroids. It can be observed that the detected position of the centroid is quite accurate in the image.

Our method actually aligns the center of the detection area with the center of the focal spot by dynamically identifying the detection window of each focal spot based on the spot center. The method also detects the centorid of each focal spot using an adaptive threshold. By aligning the center of the detection area with the center of the focal spot, the influence of noise on common averaging and windowing algorithms is eliminated, and the accuracy of the algorithm is improved greatly, even the focal spot locating far from the center of the spot sub-area. By dynamically setting the detection window and adaptively selecting the threshold of each focal spot, the influences of those noises such as diffraction of the digital SHWS, instability of the light source are also reduced, and the centroid of each focal spot can be detected very accurately.

A software system has been developed for automatic centroid detection. The software can generate spot sub-areas, detect the centers of spots, identify the detection windows, and calculate the centroids automatically. The only parameters that need to be input are the size of spot sub-area, the position of the first spot area, the intensity level of threshold and the size of detection window. The size of spot sub-area and the position of the first spot sub-area are very easy to be defined on the image, and will not affect the accuracy of centroid detection. The selections of the intensity level of threshold and the size of detection window have significant influence on the detection accuracy of the spot centroid. However, the proposed centroid algorithm is certainly convergent for these two parameters. The algorithm can detect the centroid accurately and robustly as long as these two parameters are set to some reasonable values which are big enough to cover the whole spot.

III. Experiment Results

A. Repeatability Experiment

We compare our centroid detection algorithm, which is referred to auto centroid algorithm, with some other commonly used algorithms such as statistical averaging, thresholding and windowing algorithms.

The same spot sub-area generated by the auto centroid algorithm is set as the detection area of the averaging and thresholding algorithms. The detection area of the windowing algorithm is defined to have the same size as the detection window used in the auto centroid algorithm, and be centered at the brightest pixel of each spot sub-area. The threshold used in the threshloding algorithm is set to $0.3I_{max}$, here I_{max} is the brightest intensity value in the spot sub-area.

Table 1 shows the quantitative results of centroid detection by these 4 algorithms. The X and Y coordinates of 3 centroids detected for the spot (0, 0), (3, 3) and (5, 5) are shown in the Table 1, respectively. The index of the spot is shown at the corner of each spot sub-area in the image.

At the above measurement, the position of the first spot sub-area is set as the default position (0, 0). Now, we reset the position of the first sub-area to (20, 20), so that all the spot sub-areas shift 20×20 pixels. Then we detect the centroids using 4 algorithms again, and show the results in Table 2. The coordinates of the centroids detected for the same spot, as well as their differences compared with the above measurement, are shown in Table 2. The last 2 columns show the mean differences of all the centroids in the image. We can know for the experiments that the auto centroid algorithm has better accuracy and repeatability compared with other centroid detection algorithms

TABLE I
COORDINATES OF THE CENTROIDS DETECTED BY AUTO, AVERAGING, THRESHOLDING AND WINDOWING ALGORITHMS

	Spot (0, 0)		Spot (3, 3)		Spot (5, 5)	
	X (pixel)	Y (pixel)	X (pixel)	Y (pixel)	X (pixel)	Y (pixel)
Auto	57.496	71.889	241.829	244.320	426.525	417.345
Ave	49.202	48.829	239.136	236.788	428.874	424.219
Thres	57.229	67.861	242.781	243.908	427.597	416.236
Win	57.541	72.478	240.599	244.498	425.596	417.515

B. Stability Experiment

We also study on the stability of 4 algorithms. We have conducted experiments on the digital SHWS with different light source such as white light, laser diode and He-Ne laser. Here we use laser diode as the example to demonstrate the stability of centroid detection algorithms, because compared with other two sources, laser diode is most unstable, and will introduce more noise into focus spot images.

36 images are generated by the digital SHWS within 6 hours, one image per 10 minutes. All the parameters are the same as that used in the repeatability experiment, except the threshold used in the thresholding algorithm is adjusted to $0.5I_{max}$, in order to further reduce the influence of the diffraction noise. The mean and stand deviation of the centroids detected by 4 algorithms are calculated, respectively. Table 3 shows the calculation results for 3 centroids detected for the spot (0, 0), (3, 3) and (5, 5). The last 2 columns show the overall stand deviations of X and Y coordinates of centroids calculated from all the spots in all the images.

We also use the following method to study the stability of the algorithms. We take the first image as the reference, and calculate the difference of the centroids between the first image and the subsequent image as the centroid shift.

$$S_{ij} = abs(C_{i1} - C_{ij}) \quad (4)$$

TABLE II
COORDINATES OF THE CENTROIDS DETECTED BY AUTO, AVERAGING, THRESHOLDING AND WINDOWING ALGORITHMS AFTER THE SPOT AREAS SHIFT 20×20 PIXELS, AS WELL AS THEIR DIFFERENCES COMPARED WITH TABLE 1

		Spot (0, 0)		Spot (3, 3)		Spot (5, 5)		mean	
		X (pixel)	*Y* (pixel)	*X* (pixel)	Y (pixel)	*X* (pixel)	*Y* (pixel)	*X* (pixel)	*Y* (pixel)
Auto	Cen	57.496	71.889	241.829	244.320	426.524	417.345	-	-
	Diff	0.000	0.000	0.000	0.000	0.001	0.000	0.006	0.005
Ave	Cen	69.029	68.705	258.952	256.373	448.996	444.163	-	-
	Diff	19.827	19.876	19.816	19.585	20.122	19.945	19.085	18.784
Thres	Cen	57.647	68.183	244.555	246.455	433.871	424.379	-	-
	Diff	0.418	0.322	1.845	2.547	6.274	8.143	2.631	5.107
Win	Cen	57.541	72.478	240.599	244.498	425.596	417.515	-	-
	Diff	0.000	0.000	0.000	0.000	0.000	0.000	0.000	0.000

TABLE III
MEAN AND STAND DEVIATION OF THE COORDINATES OF CENTROIDS DETECTED BY AUTO, AVERAGING, THRESHOLDING AND WINDOWING ALGORITHMS FROM 36 IMAGES

		Spot (0, 0)		Spot (3, 3)		Spot (5, 5)		overall	
		X (pixel)	Y (pixel)	X (pixel)	Y (pixel)	X (pixel)	Y (pixel)	X (pixel)	Y (pixel)
Auto	Mean	61.919	69.516	245.701	244.954	429.126	419.781	-	-
	STD	0.079	0.027	0.071	0.030	0.074	0.023	0.078	0.027
Ave	Mean	49.111	48.337	239.156	237.077	428.901	424.161	-	-
	STD	0.012	0.745	0.018	0.864	0.010	1.025	0.015	0.876
Thres	Mean	61.921	69.506	245.689	244.953	429.116	419.786	-	-
	STD	0.076	0.029	0.074	0.032	0.083	0.025	0.634	2.910
Win	Mean	61.532	69.401	245.592	244.601	428.496	419.486	-	-
	STD	0.009	0.306	0.015	0.376	0.007	0.315	0.208	0.335

where, S_{ij} is the centroid shift for the i^{th} spot in the j^{th} image. C_{i1} is the centroid of the i^{th} spot in the first image. C_{ij} is the centroid of the i^{th} spot in the j^{th} image. Then the mean centroid shift of the whole image is calculated as follows.

$$S_j = \frac{1}{N}\sum_{i=1}^{N} abs(C_{i1} - C_{ij}) \qquad (5)$$

here S_j is the mean centroid shift of all the spots in the j^{th} image. N is the number of spots in the image. The mean centroid shifts of 36 images calculated for 4 algorithms are shown in Fig. 6. We can see that the centroid shift caused by all kinds of noise such as diffraction, instability of the light source etc, is negligible for the auto centroid algorithm, which is within 0.2pixle, or 1.6μm since the pixel size of the CCD is 8μm. But it is significant for the thresholding algorithm even we have set the threshold to a quite high value.

Our experiments with the digital SHWS have demonstrated that the auto centroid algorithm has very good accuracy and stability for centroid detection from images with diffractive noise. Actually, the auto algorithm also performs quite well for general SHWS and HWS, even the quality of the image is not good. Fig. 7 shows the detected centroids by the auto algorithm from a spot image generated by a HWS, in which 25×25 micro hole array steel aperture is used. This image is quite noisy due to imperfect fabrication quality of the aperture.

In addition, the auto algorithm employs some image processing techniques which are simple and easy to be implemented. So the processing speed of the algorithm is very fast. In our experiment, the whole process of an image with the resolution of 768×572 can be completed within 100ms on a 3.20GH Pentium 4.

IV. CONCLUSION

Shark-Hartmann Wavefront sensor splits the incident wavefront into many subsections and transfers the distorted wavefront detection into the centroid measurement. The accuracy of the centroid measurement determines the accuracy of the SHWS. A lot of methods have been

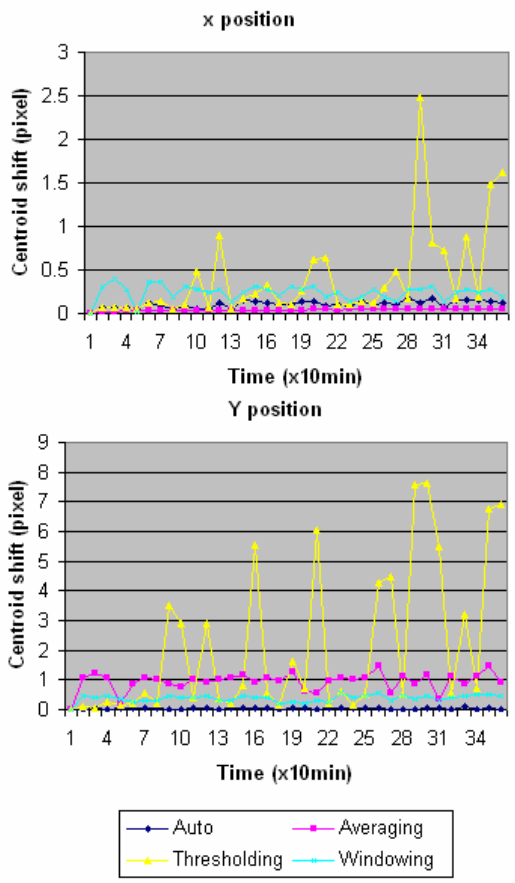

Fig. 6. Centroid shifts between the first image and subsequent images.

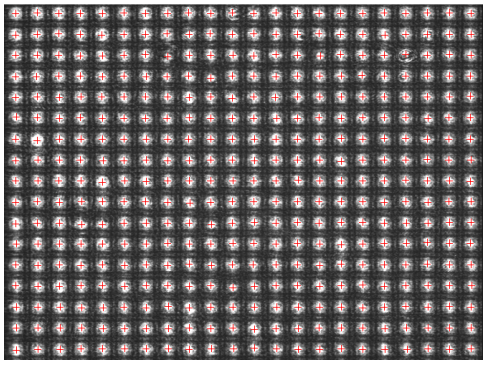

Fig. 7. Detected centroids by the auto algorithm from a spot image generated by a Hartmann Wavefront Sensor

presented to improve the accuracy of the wavefront centroid measurement. However, most of these methods are discussed from the point of view of optics, and based on the assumption that the spot intensity of the SHWS has a Gaussian distribution, which is not applicable to the digital SHWS. In this paper, we have presented a new centroid measurement algorithm based on adaptive thresholding and dynamic windowing method by utilizing image processing techniques. The method can detect the centroid of the spot accurately and robustly by eliminating the influences of various noises such as diffraction of the digital SHWS, instability of the light source as well as deviation between the centroid of the spot and the center of the detection area.

In our method, we determine the sub-area of each spot on the image directly without need to know the physical properties of the lenset array. Then we detect the spot and calculate the center of the spot using image processing techniques. After that, we dynamically identify the detection window of each focal spot based on the focal spot center, and measure the centroid of each focal spot using a threshold adaptive to the intensity distribution of that spot sub-area.

A software system has been developed for automatic implementation of the algorithm. We have studied the influence of the input parameters on the accuracy of the centroid detection, and concluded that the selection of the parameters would not affect the accuracy of the centroid as long as these parameters are set to some reasonable values which are big enough to cover the whole spot.

We also conducted repeatability and stability experiments on the proposed algorithm, and compared the performance of the algorithm with other commonly used algorithms such as statistic averaging, thresholding and windowing algorithms. The experimental results demonstrate the presented algorithm has better accuracy, repeatability and stability. The algorithm also performs quite well for general SHWS and HWS, even the quality of the image is not good.

REFERENCES

[1] T. J. Kane, B. M. Welsh and C. S. Gardner, "Wavefront detector optimization for laser guided adaptive telescope" *Proc SPIE*, 1114, pp. 160-171, 1989.

[2] G. Cao and X. Yu, "Accuracy analysis of a Hartman-Shark wavefront sensor operated with a faint object". *Opt. Eng*, 33(7), pp. 2332-2335, 1994.

[3] R. Irwan and R. G. Lane, " Analysis of optimal centroid estimation applied to Shack-Hartmann sensing", *Applied Optics*, 38, pp. 6737-6743, 1999.

[4] A. Zhang, C. Rao, Y. Zhang and W. Jiang, "Sampling error analysis of Shack-Hartmann wavefront sensor with variable subaperture pixels", *Journal of Modern Optics*, 51(5), pp. 2267-2278, 2004.

[5] S. K. Park and S. H. Baik, "A study on a fast measuring technique of wavefront using a Shack-Hartmann sensor", *Optics & Laser Technology*, 34, pp. 687-684, 2002.

[6] J. F. Ren, C. H. Rao and Q. M. Li, "An adaptive threshold selection method for Hartmann-Shack wavefront sensor", *Opto Electron Eng*, 29(1), pp. 1-5, 2002.

[7] S. H. Baik, S. K. Park, C. J. Kim and B. Cha, "A center detection algorithm for Shack-Hartmann sensor", *Optics & Laser Technology*, 39(2), pp. 262-267, 2007.

[8] P. Arulmozhivarman, L. Praveen Kumar and A. R. Ganesan, "Measurement of moments for centroid estimation in Shark-Hartmann wavefront sensor – a wavelet-based approach and comparison with other methods", *Optik*, 117, pp 82-87, 2006.

[9] S. A. Sallberg, B. M. Welsh, and M. C. Roggemann, "Maximum a *posteriori* estimation of wave-front slopes using a Shack–Hartmann wave-front sensor," *J. Opt. Soc. Am. A*, 14, pp. 1347-1354, 1997.

[10] M. A. van Dam and R. G. Lane, "Wave-front slope estimation," *J. Opt. Soc. Am. A* 17, pp. 1319-1324, 2000.

[11] J. Ares and J. Arines, "Influence of thresholding on centroid statistics: full analytical description", *Applied optics*, 43(31), pp. 5796- 5805, 2004.

[12] Z. L. Jiang, S. S. Gong and Y. Dai, "Numerical study of centroid detection accuracy for Shack-Hartmann wavefront sensor", *Optics & Laser Technology*, 38, pp. 614-619, 2006.